Russian Journal of General Chemistry, Vol. 74, No. 5, 2004, pp. 781–786. Translated from Zhurnal Obshchei Khimii, Vol. 74, No. 5, 2004, pp. 849–854.

Interactions of Copper(I) Phenanthroline Chelate with Polyadenylic–Polyuridylic Acid in Aqueous Dioxane

A. G. Kudrev

St. Petersburg State University, St. Petersburg, Russia

Received February 20, 2003

Abstract — Acid–base transformations in the system copper(I) phenanthroline chelate $[Cu(phen)_2]^+_{aq}$–polyadenylic–polyuridylic acid in aqueous dioxane were studied by spectrophotometry. Changes in band intensities and positions were revealed in the visible and near UV regions, dependent on the pH of the solution. Factor analysis was used to show that the absorption variance on titration of copper(I) bisphenanthroline chelate is determined by mutual transformations of three spectral forms of complexes. Concentration profiles were calculated for compounds prevailing in the solution. In the presence of polyadenylic–polyuridylic acid, an additional spectral form appears as a result of a short-wave shift of the d–π* MLCT transition in the copper(I) chelate complex. Analysis of the calculated concentration profiles established that the new complex is formed at pH 5.2–5.6 from the bisphenanthroline chelate and the double-helix rod-like form of the polymer.

Interactions of biopolymers with copper phenanthroline complexes and related coordination compounds containing heterocyclic bases are being studied with the aim to develop on their basis specific reagents for purposive modification of the composition and structure of nucleic acids [1–3]. Such reagents affect the ability of a polynucleotide to interact with other components and function as active restrictases [4, 5]. The effect of copper(I) phenanthroline complexes on DNA and RNA is well-documented [1–5]. A number of structural models of the DNA–$[Cu(phen)_2]^+$ complex have been substantiated on the basis of experimental evidence. The present notion relies on the concept of intercalation of metal chelates into hydrophobic segments of DNA. With copper bischelate compounds, partial intercalation with accommodation of the second ligand in the minor groove of the biopolymer is proposed. This model readily explains why copper 1,10-phenanthroline bischelates interact with DNA and RNA, whereas 2,9-dimethyl-1,10-phenanthroline chelates no. The case in point here is that in the first case the dihedral angle between the ligands is close to the slope of the minor groove to the nucleic base plane, while in the second, the mentioned angles are quite different.

The restrictase activity of copper(I) phenanthroline complexes has been rather well studied on a qualitative level, but the quantitative information on the stability of complexes with these chelates capable of inducing DNA and RNA degradation is very scarce [6, 7]. It is considered that addition of $[Cu(phen)_2]^+_{aq}$ to DNA plays an important role in *in situ* degradation of the biopolymer. The copper(II) complex is formed by oxidation of Cu(I) or is present in the initial solution. DNA inhibits Cu(II) reduction [6]. As follows from the kinetic model, the Cu(II) complex DNA–$[Cu(phen)_2]^{2+}_{aq}$ (K_{st} 1.8×10^4 [6], 3.7×10^4 [7]) is much less stable that the Cu(I) complex DNA–$[Cu(phen)_2]^+_{aq}$ (K_{st} 2×10^5 [7]).

The aim of the present work was perform a spectrophotometric study of interactions of the copper(I) chelate complex $[Cu(phen)_2]^+_{aq}$ with synthetic polyadenylic–polyuridylic acid in equilibrium conditions. The chosen biopolymer is a double-helix polyribonucleotide, similar in shape to natural DNA [8].

Mathematic treatment of spectrophotometric titration results. Quantitative analysis of variable-pH spectral measurements in the system chelate complex–polymer was performed in terms of the so-called "soft" model [9]. In each experimental point, absorbance data (spectrum) was obtained at the same number of wavelengths. This approach allowed an augmented general matrix **A** to be constructed, which combines the results of separate titrations A_i [Eq. (1)].

$$\mathbf{A} = [A_1;\ A_2 ... A_n]. \quad (1)$$

Calculation of the number of factors R, determining the variance of the augmented matrix ***A.*** The calculation of R was performed by the principal component analysis (PCA) [10–12] using the singular value decomposition procedure [13]. SVD allows a matrix to be recovered with a set of independent variables whose number is equal to the rank of data

1070-3632/04/7405-0781 ©2004 MAIK "Nauka/Interperiodica"

matrix **A** and the number of principal factors *R*, according to Eq. (2).

$$\mathbf{A} = \mathbf{USV}^T + \tau = \mathbf{A}^* + \tau. \quad (2)$$

Here **U** and **V** are orthogonal matrices, **S** is a diagonal matrix, **A*** is a matrix recovered with *R* factors, and τ is the recovery error. Obviously. Eq. (2) is valid if the recovery error is smaller than the experimental error. By the PCA method the rank can be determined from a comparison of the experimental data matrix and the matrix recovered from SVD results for a model including *R* factors.

To compare matrices of the same size, in the present work we made use of the Hamilton factor. At similar measurement errors, the weight coefficients in the Hamilton equation can be neglected and percent matrix divergence can be calculated [Eq. (3)].

$$E(\mathbf{A}, \mathbf{A}^*) = \left(\frac{\mathbf{Tr}\{(\mathbf{A}^* - \mathbf{A})(\mathbf{A}^* - \mathbf{A})^T\}}{\mathbf{Tr}\{(\mathbf{AA}^T\}} \right) \times 100\%. \quad (3)$$

Here **A** and **A*** are the matrices to be compared and **Tr** is the matrix trace. The lowest *R* number at which the $E_{\mathrm{SVD}}(\mathbf{A}, \mathbf{A}^*) < 100\sigma$ condition is met is taken to be equal to the matrix rank, and σ is the experimental error.

The rank was also calculated by means of the *t*-statistics by Eq. (4).

$$t = U \times E \times inv(diag\sqrt{\lambda_i}\ ). \quad (4)$$

Here $diag\sqrt{\lambda_i}$ is a diagonal matrix with elements $\sqrt{\lambda_i}$; λ_i are eigenvalues of matrix **A**, and *inv* is the matrix reversal sign. The critical value of the *t*-statistics is calculated by Eq. (5).

$$t^2_{\mathrm{lim}} = [R(m - 1)/(m - R)]F(\alpha, R, m - R). \quad (5)$$

Here *m* is the number of experimental points, *R* is the number of principal components (the number of degrees of freedom of the larger variance), *F* is the tabulated *F*-distribution value, and *m*–*R* is the number of degrees of freedom of the smaller variance, confidence probability α 0.05.

Transformation of abstract factors into variables having a physicochemical meaning. In spectrophotometric studies, to transform the abstract factors calculated by Eq. (2) into factors having a physicochemical meaning, one should perform the corresponding rotation in the vector space to transform matrix $\mathbf{V}^T$ into a spectra matrix **E**. If a system includes some selectivity, then to matrix $\mathbf{V}^T$ corresponds a matrix of *R* least correlated rows of matrix **A**. Matrix **US** should be transformed into a concentration profiles matrix that allows recovery, within the experimental error, of the original data matrix by Eq. (1). Let us white down the calculation of concentration profiles matrix **C** as a matrix division operator [Eq. (6)].

$$\mathbf{C} = \mathbf{A/E}. \quad (6)$$

With matrix **C**, we can calculate a refined spectra matrix by the operator given by Eq. (7).

$$\mathbf{E} = [\mathbf{A}^T/\mathbf{C}^T]^T. \quad (7)$$

Alternating least-squares optimization. In the ALS–MCR analysis of augmented matrices, as the initial approximation we took spectra calculated for the subsystems. Iterative solution of operators (6) and (7) gives optimal, in terms of the least-squares method, $\mathbf{C}_i$ and $\mathbf{E}_i$ values, where *i* is the number of the experimental data matrix. The concentration and spectral profiles for systems including selectivity are calculated to a high accuracy [14]. In the absence of selectivity, the utility of ALS optimization may prove limited [15]. The fit of calculated concentration profiles to experimental can be improved. For example, one make use of "soft" constraints [16–18] (unimodality of concentration profiles **C**, nonnegativeness of **C** and **E**, etc.) or "hard" constrains [19, 20] (fulfillment of mass balance equations and mass action law) in the ALC–MCR procedure. Correct application of the above constrains generally allows one to lift rotational uncertainty and, for certain titrations in cases where the experimental error fits the normal law, to calculate statistical expectations for **C** and **E** [21].

Acid–base behavior of copper(I) bisphenanthroline chelate. Preliminary experiments showed that the electronic absorption spectra are quite sensitive to the total concentration ratio of copper and phenanthroline in the solution. This brings up an additional variance in measurement results if the Cu–Phen ratio is set, gravimetrically or by aliquots, directly in the solution. A constant [Cu]/[Phen] ratio of 1 : 2 can be provided by using the corresponding copper complex. This eliminates errors associated with component concentration ratio but creates certain difficulties with qualitative interpretation of acid–base titration results.

The plot of the absorbance of $[Cu(phen)_2]^+$ solution (c_{tot} 1.3×10^{-4} M) at λ 430 nm vs. pH is shown in Fig. 1. As seen from the titration curve, at least two equilibrium processes take place in the pH range studied, which are responsible for the increase and subsequent decrease of the optical density.

Variance in the experimental data matrices **A**, described by the PCA method, %

Principal component no.	Eigenvalue of the matrix		Variance described by the principal component, %		Variance described by the sum of principal components, %	
	$[A_1;\ A_2]$	$[A_1;\ A_2;\ A_3]$	$[A_1;\ A_2]$	$[A_1;\ A_2;\ A_3]$	$[A_1;\ A_2]$	$[A_1;\ A_2;\ A_3]$
1	1.56×10^{1}	1.44×10^{1}	98.5	98.1	98.5	99.1
2	2.42×10^{-1}	2.79×10^{-1}	1.52	1.89	99.99	99.97
3	9.37×10^{-4}	3.22×10^{-3}	0.01	0.02	100.0	100.0
4	7×10^{-4}	2.25×10^{-4}	0.00	0.003	100.0	100.0
5	2×10^{-5}	1×10^{-4}	0.00	0.00	100.0	100.0
6	6×10^{-6}	3×10^{-5}	0.00	0.00	100.0	100.0

We performed a PCA analysis of the submatrix of general absorbance matrix $\mathbf{A}_{1,2} = [A_1; A_2]$ constructed of two independent titration results. The results of the analysis are presented in the table and Fig. 2.

As seen from the table, the absorbance variance is fully described by three principal factors. From this it follows that changes in the absorption spectra are determined by interconversions of three spectral forms. But, according to the "hard" model [22], the complex formation of copper(I) with phenanthroline at a 1:2 metal–ligand ratio in the course of titration involves four chemical forms. The result of the "soft" modeling can be explained in terms of rotational uncertainty.

The distribution of the forms as a function of pH is shown in Fig. 3. The same figure shows the profiles of abstract spectral forms, calculated by the ALS–MCR procedure from the general experimental matrix $\mathbf{A}_{1-3}$. Comparing the profiles obtained by the "hard" and "soft" models one can see that the fractions of spectral forms *1* and *2* change in parallel with the relative concentrations of $[phenH]^+$ and $[Cu[phen)_2]^+$. The shapes of the calculated spectra of forms *1* and *2* (Fig. 3b) provide evidence for this assignment. The spectrum of form *1* contains nothing more than the long-wave boundary of the absorption due to phenanthroline $n\rightarrow\pi^*$ and $\pi\rightarrow\pi^*$ transitions. The spectrum of form *2* contains, along with this absorption, a band in the regions characteristic of the $d\rightarrow\pi^*$ MLCT transition characteristic of copper(I) chelate complexes with heterocyclic diamines. The pH dependence of the concentration of form *3* best correlates with the respective dependence for [phen]. However, the spectrum of this form contains a strong MLCT band. Taking this into account and for chemical reasons we can admit the absorbance variance a described by spectral form *3* is a linear combination of the changes in the concentrations of [phenH] and $[Cu(phen)_2]$. The aforesaid suggests that the rotational uncertainty can be described by Eq. (8).

$$\mathbf{A} = \varepsilon_{Cuphen}[Cu(phen)] + \varepsilon_{Cuphen_2}[Cu(phen)_2] + \varepsilon_{phen}[Phen] + \varepsilon_{phenH}[phenH] = \varepsilon_1[1] + \varepsilon_2[2] + \varepsilon_3[3]. \quad (8)$$

Effect of Poly(A)–Poly(U) additives. Figure 1 shows the plot of the absorbance of the $[Cu(phen)_2]^+$ solution at λ 430 nm vs. pH in the presence of Poly(A)–Poly(U) (c_{tot} 1.8×10^{-4} M). Absorbance measurements were performed at various pH, and, therefore, nonlinear interpolation is needed for comparable titration curves. In the present work we made use of polynomial interpolation. Seventh degree polynomial nicely fits the titration curves in their common range of arguments (pH 3.2–5.9). The divergence of vectors in independent of the number of arguments and comprises 6% for polynomials calculated from *A*–pH dependences without Poly(A)–Poly(U) additives. The $PE_{1,2}$ value of 6% is in essence the experimental error. The mean divergence between the *A*–pH dependences with and without Poly(A)–Poly(U) addi-

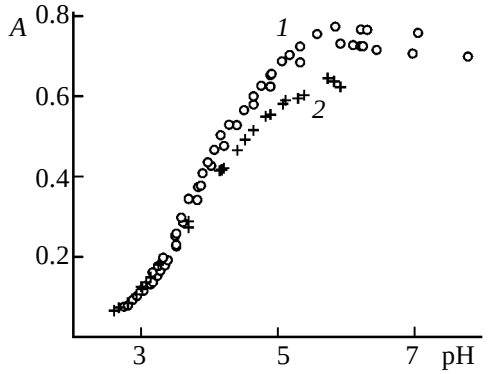

Fig. 1. Plot of the absorbance of the $[Cu(phen)_2]^+_{aq}$ solution at λ 430 nm vs. pH. (*1*) Without additives and (*2*) with Poly(A)–Poly(U) additive.

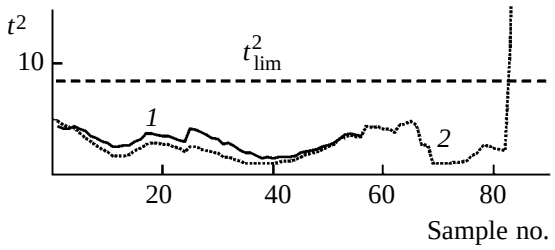

Fig. 2. Values of the t^2-statistics for the (*1*) [A_1; A_2] and (*2*) [A_1; A_2; A_3] matrices; t^2_{lim} is the limiting value for the three-factor model.

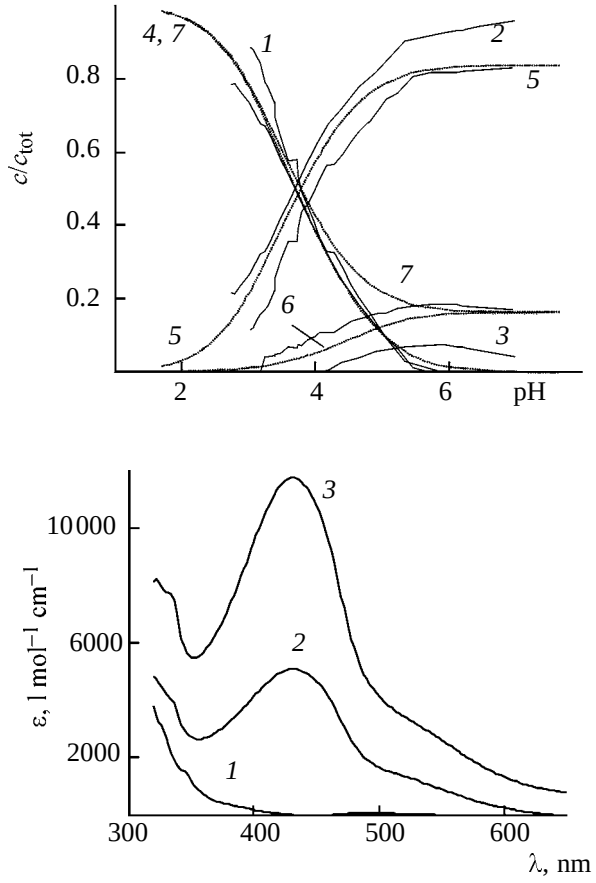

Fig. 3. Results of the ALS–MCR decomposition of the [A_1; A_2] matrix. (a) (*1*–*3*) [c_1, c_2]/c_{tot}[Cu(phen)$_2$] matrix (relatives contents of complex forms *1*–*3*; dotted lines relate to the theoretical model); (*4*) [phenH]$^+$, log K_{st} 4.95; (*5*) [Cu(phen)$_2$], log K_{st} 15.8; (*6*) [phen]; and (*7*) [Cu(phen)]$^+$, log K_{st} 10.3. (b) [S]/c_{tot}[Cu(phen)$_2$] matrix (absorption spectra of forms *1*–*3*).

tives is 12% [($PE_{1,3}$ + $PE_{2,3}$)/2]. Similar significant divergences are observed at other wavelengths. The observed divergence in titration curves is largely explained by various relative contents of the principal spectral forms.

As seen from the table, the absorbance variance in the presence of Poly(A)–Poly(U), too, is determined by three principal factors. Analysis of the t^2-statistics (Fig. 3) shows that the three-factor model fits almost all experimental points, except for a number of extreme points at the highest pH values. Further increase of pH enhances wavelength-independent light scattering and then precipitate formation. Apparently, the observed jump in the t^2-statistics is associated with the initial stage of the process, implying formation of a new compound in the Poly(A)–Poly(U)–[Cu(phen)$_2$]$^+_{aq}$ system.

Comparison of the pH dependences of the relative contents of forms for Poly(A)–Poly(U) + [Cu(phen)$_2$]$^+_{aq}$ (Fig. 4) and Poly(A)–Poly(U) [23] (Fig. 5) shows that form *4* appears in the same pH range as the protonated form *3* of the polynucleotide begins to form.

The latter form is a double-helix RNA with fully deprotonated adenine bases and protonated uridine bases [23]. This form of RNA is considered to be stretched as a rod [8]. Such conformations renders the central (hydrophobic) segment of the biopolymer the most accessible for interactions with foreign reagents. Once the content of this form of Poly(A)–Poly(U) has attained 60%, the concentration of [Cu(phen)$_2$]$^+_{aq}$ begins to decrease sharply, implying that the complex formation is cooperative in nature. As seen from Figs. 3 and 4, the polynucleotide additive affects the concentration profiles making them appreciably different from those expected by additivity. A new spectral form *4* appears and the formation of form *3* is almost completely suppressed. A little form *3* is only formed at pH ~5.5, i.e. in the range of Poly(A)–Poly(U)–[Cu(phen)$_2$]$^+_{aq}$ formation onset. This fact suggests that no free phenanthroline and [Cu(phen)]$^+$ are present in the system at pH > 5.6. The absence of phenanthroline and [Cu(phen)$_2$]$^+_{aq}$ is explicable in terms of stabilization of the bischelate [Cu(phen)$_2$]$^+_{aq}$ due to hydrophobic π_{Poly}–π_{phen} interactions.

According to the aforesaid, the observed changes in the absorption spectra are explained by the formation at pH 5.2–5.6 of a new complex between the bisphenanthroline chelate and the double-helix rodlike form of the polymer.

EXPERIMENTAL

Synthetic Poly(A)–Poly(U) (Sigma), NaCl, NaOH, HCl, and ascorbic acid (Merck) were used as received. Solutions were prepared with a mixture of distilled water and dioxane in a 4 : 1 ratio. The copper bisphenanthroline complex was synthesized by the fol-

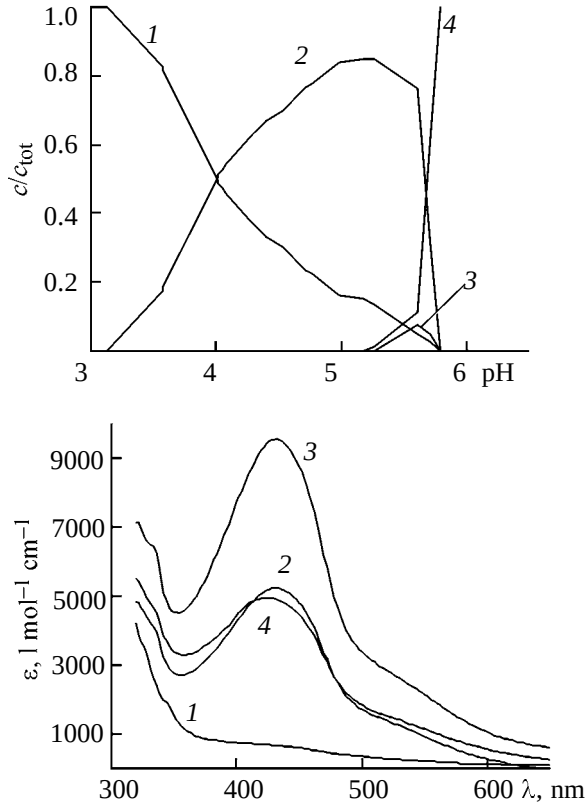

Fig. 4. Results of the ALS–MCR decomposition of the $[A_1; A_2; A_3]$ matrix. (a) (*1*–*3*) $[c_3]/c_{tot}[Cu(phen)_2]$ matrix (relative contents of forms *1*–*3*); and (*4*) [Poly(A)–Poly(U)]–$[Cu(phen)_2]$. (b) $[S]/c_{tot}Cu(phen)_2]$ matrix (absorption spectra of forms *1*–*4*).

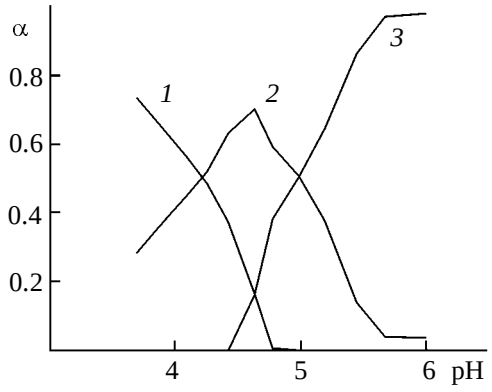

Fig. 5. Plot of the relative contents of forms of polyadenylic–polyuridylic acid vs. pH. (*1*) Poly(AH)–Poly(UH), (*2*) Poly(AH*)–Poly(UH), and (*3*) Poly(A)–Poly(UH).

lowing procedure. 1,10-Phenanthroline was added to a solution of $CuCl_2 \cdot 2H_2O$ in aqueous dioxane (reagent ratio 2 : 1). The solvent was evaporated, and the residue was filtered off and washed with cold water. The elemental composition of $Cu(phen)_2Cl_2 \cdot H_2O$ was determined on a Perkin–Elmer automatic analyzer. Found, %: C 56.9; H 3.7; N 10.5. $Cu(phen)_2Cl_2 \cdot H_2O$. Calculated, %: C 56.2; H 3.5; N 10.9.

The UV spectra were measured on a Perkin–Elmer Lambda-19 spectrophotometer combined with PC. Absorbance measurements were performed in the range 320–650 nm with 2 nm increments. The temperature (37°C) in the spectrophotometric cell was maintained with a device utilizing the Peltier effect. Titration and pH measurements were performed using an Orion-701A pH meter in a temperature-controlled cell at 37C in a 0.15 M aqueous-dioxane solution of NaCl under N_2. A stream of N_2 was passed through the initial titrate and alkali solutions for 2 h, and the titrate was then mixed with ascorbic acid directly in the cell not exposing it to air. After a further portion of alkali had been added and pH measured, the solution was pumped over into a hermetic spectrophotometric cell by means of a peristaltic pump in air-proof conditions.

REFERENCES

1. Tullius, T.D., *Metal–DNA Chemistry*, Tullius, T.D., Ed., Washington: Am. Chem. Soc., 1989, pp. 1–47.
2. Sigman, D.S., Mazumber, A., and Perrin, D.M., *Chem. Rev.*, 1993, vol. 93, no. 6, p. 2295.
3. Papavassilion, A.G., *Biochem. J.*, 1995, vol. 305, no. 2, p. 345.
4. Pogozelski, W.K. and Tullius, D.T., *Chem. Rev.*, 1998, vol. 98, no. 3, p. 1089.
5. McMillin, D.R. and McNett, K.M., *Chem. Rev.*, 1998, vol. 98, no. 3, p. 1201.
6. Thederahn, B.T., Kuwabara, M.D., Larsen, T.A., and Sigman, D.S., *J. Am. Chem. Soc.*, 1989, vol. 111, no. 13, p. 4941.
7. Goldstein, S. and Czapski, G., *J. Am. Chem. Soc.*, 1986, vol. 108, no. 9, p. 2244.
8. Saenger, W., *Principles of Nucleic Acid Structure*, New York: Springer, 1984.
9. Kudrev, A.G., *Zh. Neorg. Khim.*, 2001, vol. 46, no. 5, p. 854.
10. Malinowsky, E.R. and Howery, D.G., *Factor Analysis in Chemistry*, New York: Wiley, 1980.
11. *Computer Aids to Chemistry*, Vernin, G. and Chanon, M., Eds., Chichester: Horwood, 1986. Translated under the title *EVM pomogaet khimii*, Leningrad: Khimiya, 1990, pp. 182–237.
12. Hugus, Z.Z. and El-Awady, A.A., *J. Phys. Chem.*, 1971, vol. 75, no. 19, p. 2954.
13. Golub, G.H. and Van Loan, Ch. F., *Matrix Computations*, London: The Johns Hopkins Univ. Press, 1989.

14. Mane, R., *Chemom. Intell. Lab. Systems*, 1995, vol. 27, p. 89.

15. Tauler, R., Smilde, A., and Kowalski, B., *J. Chemometrics*, 1995, vol. 9, p. 31.

16. Tauler, R. and Casassas, E., *Analysis*, 1992, vol. 20, p. 255.

17. Tauler, R., Izquierdo-Ridorsa, A., and Casassas, E., *Chemom. Intell. Lab. Systems*, 1993, vol. 18, p. 293.

18. de Juan, A., Vander Heyden, Y., Tauler, R., and Massart, D.L., *Anal. Chim. Acta*, 1997, vol. 346, p. 307.

19. Gampp, H., Maeder, M., Meyer, C.J., and Zuberbuhler, A.D., *Talanta*, 1985, vol. 32, p. 1133.

20. Gampp, H., Maeder, M., Meyer, C.J., and Zuberbuhler, A.D., *Talanta*, 1986, vol. 33, p. 943.

21. Kudrev, A.G., *Koord. Khim.*, 1999, vol. 25, no. 2, p. 152.

22. Sillen, L.G. and Martel, A.E., *Stability Constants of Metall-Ion Complexes*, London: Chem. Soc. Burlington House, 1964.

23. Kudrev, A., Gargallo, R., Izquierdo-Ridorsa, A., Tauler, R., and Cassassas, E., *Anal. Chim. Acta*, 1998, vol. 336, no. 1, p. 119.